SLAC – PUB – 4227
June 1987
(A)

BEAM DYNAMICS IN THE SLC FINAL FOCUS SYSTEM*

P. S. BAMBADE

Stanford Linear Accelerator Center
Stanford University, Stanford, California 94305

Abstract

The SLC luminosity[1] is reached by colliding beams focussed to about 2 μm transverse sizes. The Final Focus System (FFS) must enable, beyond its basic optical design,[1,2] the detection and correction of errors accumulated in the system. In this paper, after summarizing the design, we review the sensitivity to such errors and the ability to correct them. The overall tuning strategy involves three phases: single beam spot minimization, steering the beams in collision and luminosity optimization with beam-beam effects.

Summary of Optical Design[1,2]

Focussing the beam to a small transverse size would be easy if the input phase space (transverse emittance and energy spread) were small enough. A *monoenergetic* beam with horizontal emittance $\epsilon_x = \sigma_x^{in}\sigma_\theta^{in}$ would, for example, be focussed to $\sigma_x^* = \sigma_x^{in} l^*/L$ a distance l^* from a lens with focal length $1/f = 1/l^* + 1/L$ (see Fig. 1). In a more realistic beam with finite energy spread σ_E, rays on the edge of the energy distribution are focussed at an axial position displaced by $l^*\sigma_E$, thus adding $2l^*\sigma_E\sigma_\theta^*$ to the overall size (a factor 2 is put in since at least two lenses are used to focus both planes). This *chromatic aberration* is negligible if $\epsilon\sigma_E \leq \sigma_x^{*2}/2l^*$. In the SLC where $\sigma_x^* \simeq 1.5\mu m$, $\epsilon \simeq 3\ 10^{-10}$ mrad, $\sigma_E \simeq 0.002$ and $l^* \approx 5m$ (computed to the principle plane of the final lenses), it amounts to $\sigma_{chrom}^* \simeq 4\mu m$, and thus dominates the spot.

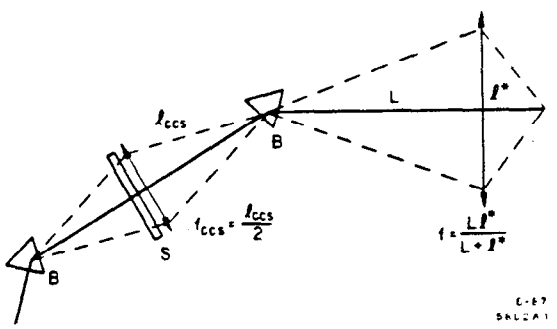

Fig. 1. A simplified Final Focus.

The resulting luminosity, computed by averaging the usual expression over the two beams' energy distributions (assumed square with half-width σ_E), is given by:

$$\mathcal{L}(\beta^*,\sigma_E) = \frac{fN^2}{2\pi\sigma_E^2}\int_0^{\sigma_E}\int_0^{\sigma_E} \frac{d\delta_E^+ d\delta_E^-}{2\epsilon\beta^* + \frac{\epsilon}{\beta^*}F^2(\delta_E^{+2} + \delta_E^{-2})} \qquad (1)$$

where $F = \sigma_x^*(\delta_E)/\sigma_\theta^*\delta_E$ is a measure of the aberration. It is shown versus β^* in Fig. 2, normalized to $\mathcal{L}(\beta_{nom}^*, \sigma_E = 0)$, for an as-built FFS with no chromatic compensation ($F \approx 15m$). Independent of ϵ, it gives the optimum β^* for such an FFS. For $\sigma_E = 0.002$ and $\beta_{opt}^* \simeq 1.5$ cm, $\mathcal{L}$ is down by a factor 3.5. This is not as low as what we get directly with the size estimate because the aberration spreads the edges of the bunch out more than its core, and because the luminosity is a sum of squares.

* Work supported by the Department of Energy, contract DE-AC03-76SF00515.

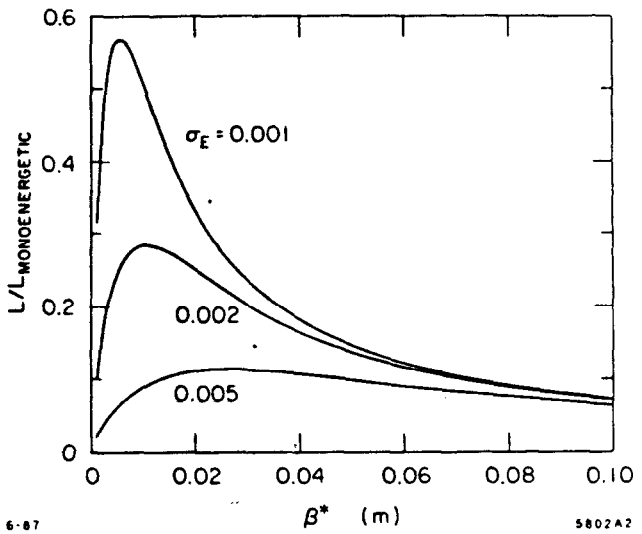

Fig. 2. Relative luminosity loss versus β^* and σ_E for a Final Focus without chromatic correction.

Compensation requires a special Chromatic Correction Section (CCS) upstream of the final lens. In a simplified CCS, two dipoles of strength B separated by $2l_{ccs}$, are imaged by a quad with focal length $l_{ccs}/2$, resulting in a 1^{st} order achromat (see Fig. 1). Near the quad is a sextupole of strength S, in which the field varies quadratically with excursion, and in which rays with energy deviation δ_E are transported off-axis. This produces a stronger overall quad for rays both off-angle and off-energy ($\theta\delta_E$ term), which offsets the weaker focussing in the final lens. Equating the contributions to σ_{chrom}^* from the final lens and from the sextupole (neglecting the CCS quad), we find that $M = l^*/L$, $R_l = l^*/l_{ccs}^2$, B and S scale like $S \propto R_l/MB$.

Unfortunately, the sextupole also deflects rays solely off-energy or off-angle, thus giving terms in θ^2 and δ_E^2. Cancelling these two new aberrations requires that the CCS be made of two consecutive and identical sections, with sextupoles in pairs π phase shift apart and sequential symmetry for the η-function. The real system,[2] designed to focus achromatically in both planes, uses telescopes, each consisting of two triplets, instead of the lenses. This minimizes[1,3] the dominant $\theta\delta_E, \phi\delta_E$ terms and suppresses the other 2^{nd} order term in $x\delta_E, y\delta_E$ while demagnifying in both planes. The chromatic correction, also done in both planes, requires two sextupole families. Coupling effects between them can significantly enhance 3^{rd} order chromatic and geometric contributions and must be minimized. The three dominant terms are $\theta\delta_E^2$, $\theta^2\delta_E$ and θ^3. Neglecting the final lenses, these terms scale like $S^2B^2\sigma_E^2\sigma_\theta^{*}M$, $S^2B\sigma_E\sigma_\theta^{*2}M^2$ and $S^2\sigma_\theta^{*3}M^3$. Substituting for the sextupole strength needed to correct, we get $\frac{R_l^2\sigma_E^2(\epsilon/\beta^*)^{1/2}}{M}$, $\frac{R_l^2\sigma_E(\epsilon/\beta^*)}{B}$ and $\frac{R_l^2M(\epsilon/\beta^*)^{3/2}}{B^2}$. For given phase-space volume, space constraints and desired β^* the overall effect of these aberrations is minimized adjusting M,B and S to balance them out. An approximate criterion[1,2] is obtained equating the two 1^{st} terms giving $\sigma_\theta^{in} = \sigma_E B$. Physically this means that monochromatic and chromatic sizes should be about equal in the sextupoles.

Invited paper presented at the 1987 Particle Accelerator Conference, Washington, D. C., March 16–19, 1987

These considerations are relevant not only to the design, but as we shall see, to the *experimental tuning strategy:* We must in effect insure proper optical matching into the CCS to maintain the optimization. The whole system is shown in Fig. 3. It includes two more sections to match the Arc lattice.

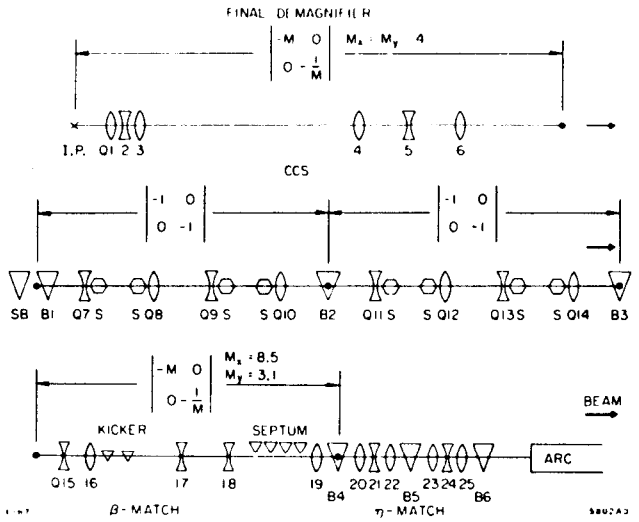

Fig. 3. Schematic of FFS.

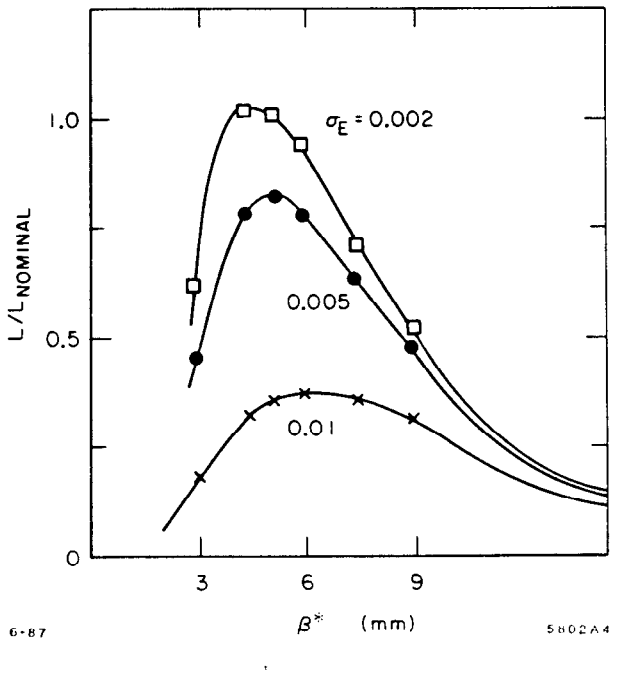

Fig. 4. Relative luminosity loss versus β^* and σ_E for a Final Focus chromatically corrected to 2^{nd} order.

Sensitivity to Optical Mismatch

In real operation, both the volume and shape of the injected phase space differ from specification because of errors, thereby increasing σ^*.

Enhancements in ϵ, from wakefields in the Linac or synchrotron radiation in the Arc, as well as an imperfectly minimized σ_E, are uncorrectable in the FFS. The damage can, however, be reduced somewhat by retuning the betatron match into the CCS. For larger ϵ, σ^* is first dominated by the 3^{rd} order $\theta^2\delta_E$ term. Varying β^* to minimize the overall $(\epsilon\beta^* + (\sigma_E\epsilon/\beta^*)^2)^{\frac{1}{2}}$ size gives $L \propto \epsilon^{-\frac{4}{3}}$ for $\beta^*_{opt} \propto \epsilon^{\frac{1}{3}}$. Similarly for σ_E (now with $\delta_E^2\theta$) we would get $L \propto \sigma_E^{-2}$ for $\beta^*_{opt} \propto \sigma_E^2$ if the bunch remained gaussian. Actual simulation (MURTLE[4]) shows close to linear loss with weak dependance on β^* (see Fig. 4).

Optical distortions from gradient errors upstream are mostly linear[5] and can be corrected within some bounds. The primary effect results from a 1^{st} set enhancing σ^* directly by correlating positions with angles or with δ_E at the IP. This amounts to axial offsets in the waists, x-y coupling ($x\phi$ or $y\theta$ terms) and anomalous $\eta_{x,y}$. The axial waist offset Δ_{waist} must be corrected to better than β^*=0.75 cm, since $\beta^*_{eff} = \beta^* + \Delta_{waist}{}^2/\beta^*$, and $\eta_{x,y}$ to better than 1 mm. A 2^{nd} set affects luminosity indirectly by perturbing the IP angular spread, through the magnitude of $< \theta^2 >$ and $< \phi^2 >$, and through anomalous $\eta_{\theta,\phi}$ and $\theta\phi$ coupling terms. Smaller spread increases β^* linearly. Inversely, a larger spread reduces it but also enhances the 3^{rd} order $\theta\delta_E^2$, $\theta^2\delta_E$ and θ^3 aberrations, as the criterion for optimal balancing is no longer satisfied. The relative luminosity loss versus β^* is shown from simulation in Fig. 4 for different σ_E. The shape is the same as in the chromatically uncorrected case in Fig. 2. Here, although the CCS has left 3^{rd} aberrations, it has removed the dominant 2^{nd} order terms, thereby raising $\mathcal{L}^{max}$ and shifting β^*_{opt} towards smaller values. The tolerance on β^* is about $\pm 20\%$. Outside this range, the spot will not have the design size even if the 1^{st} set of distortions are corrected. For β^* too large, $\mathcal{L} \propto 1/\beta^*$ from linear optics. For β^* too small, $\mathcal{L}$ falls off, first linearly, than parabolically, as it becomes dominated by 3^{rd} aberration.

Optical Corrections

The FFS could in principle be designed to fully match optical distortions generated upstream. Accumulated errors of any size would then be left for correction there. This is not feasible in the SLC because of the Arc, where minimizing synchrotron radiation induced emittance growth requires a reasonable optical match throughout. The 1^{st} step to specify the matching solution is to set tolerances for the Arc and its input match to avoid large growth. Investigating such tolerances is beyond the scope of this paper. Let us simply mention that the blowup is small[6] for random imperfections three times the specified tolerance.[7] Input mismatch and systematic errors are more damaging.

The distortion's size then determine the range over which the FFS must be tunable, and the above sensitivities how well one must match. Not all parameters are important. With no pinch effect initially and with σ_E basically set by the Linac, we consider distortions only in the four betatron dimensions and in their couplings to energy. Betatron space is described by the usual σ-matrix,[8] with ten terms σ_{ij}=$< x_i x_j >$. The R-matrix describing the lattice has 16 terms. Output phase space is related to input by $\sigma_{out} = R\sigma_{in}R^t$ where R^t is the transpose of R. For linear optics and neglecting synchrotron radiation, Poincarré invariance requires[9,10] that R be symplectic:

$$R^tSR = S, \quad \text{with} \quad S = \begin{pmatrix} 0 & -1 & 0 & 0 \\ 1 & 0 & 0 & 0 \\ 0 & 0 & 0 & -1 \\ 0 & 0 & 1 & 0 \end{pmatrix} \qquad (2)$$

thereby restricting the number of free terms in R to ten. Applying the same algebra to the σ-matrix, we find that the betatron space can only be perturbed by the optics in six independent ways. With the four dispersions $\eta_{x,\theta,y,\phi}$, we thus have a total of *ten independent distortions* to correct.

We choose to represent them by those for which tolerances were given above: the five IP angular sizes $< \theta^2 >$, $< \phi^2 >$, $< \theta\phi >$ and $\eta_{\theta,\phi}$, and the five correlations of IP positions to angles and energy $< x\theta >$,$< y\phi >$,$< y\theta >$ (or $< x\phi >$) and $\eta_{x,y}$. Ideally correction would be done upstream of the CCS, to avoid perturbing its optimization relative to the Final Demagnifier. This is possible for η, but only partially possible for betatron space.

Dispersion is corrected perturbing the η-match with four quads,[2] installed in pairs $\pi/2$ and π phase shift from the IP, to control spatial and angular η, respectively. Each pair consists of an erect and a skew quad for control in both planes. Naturally orthogonal for small input $\eta_{y,\phi}$ (the two erect ones perturbing the match of the horizontal lattice dispersion, and the two skew ones coupling it into vertical), they are coupled if it is large. Correction range is limited by quad strengths but also by the particular orientation of input η. Some specific values make them ineffective. This happens, for example, when $\eta_{x,\theta}^{anomalous}$ exactly cancels $\eta_{x,\theta}^{lattice}$. The domain of correctable $\eta_{x,\theta}$ therefore has a *dead zone* (see Fig. 5). With $\eta_{ARC}^{lattice}$ modulating around 35 mm with maximum slopes of ± 18 mrad, uncorrectable cases appear if, for instance, the horizontal betatron phase in the back of the Arc is off by a quarter of a modulation cycle with the appropriate sign. Gross control is thus required upstream to bring η within *capture range*.

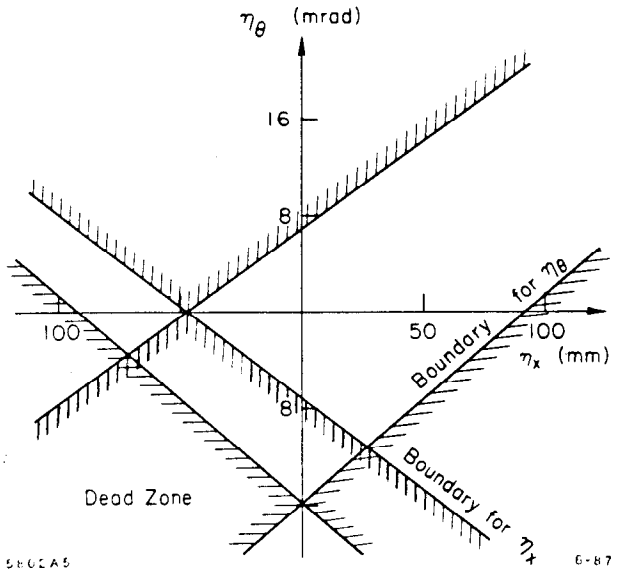

Fig. 5. Domain of correctable horizontal dispersion.

Betatron matching is split across the CCS, in the β-match and Final Demagnifier. The three angular terms $< \theta^2 >$, $< \phi^2 >$ and $< \theta\phi >$ are adjusted upstream of the CCS with two of the β-match quads and a skew quad, allowing to control the ratio of betatron to chromatic sizes in the sextupoles. The three waist offsets $< x\theta >$,$< y\phi >$ and $< y\theta >$ cannot be adjusted within the β-match independently of the angular terms. The are taken out at the very end, with two of the final lenses and a 2^{nd} skew quad. This strategy does not maintain exactly the relative optimization of the Final Demagnifier and CCS, as the last lenses are tweaked. The luminosity, somewhat derated as some 2^{nd} order aberration reappears, can be restored readjusting the sextupoles. Except for some cases of large errors, this is a small effect. With present hardware, the correction range is about $\pm 40 \times \beta^*$ for waist control (or 30 cm for $\beta^* \simeq 0.75$ cm) and a factor 3 in either direction for angular spread. Simulations and calculations show that random errors three times those expected in the Arc can be handled.

Overview of Tuning Strategy

Turning 12 coupled knobs guided only by the IP spot—let alone optimizing two colliding beams—would be very difficult without an ordered procedure. Since measuring μm-size beams is not straightforward, we must minimize the number of tuning experiments requiring IP information by diagnosing as many aspects of phase space as possible before demagnification or wherever conventional instruments are adequate.

Our tuning strategy begins with optical matching of a single beam using strip-line Beam Position Monitors (BPMs) with about 20 μm resolution and phosphor screens with about 35 μm resolution. At the IP, crude measurements are done using thin carbon wires, about 5 μm in diameter, from which spot sizes and centroids are inferred by scanning. Such wire targets and BPMs near the IP have been designed for initial commissioning, but are also part of the early detector configuration.

After both beams are minimized, they are brought and kept in collision, first with BPMs near the IP, and then exploiting the electromagnetic fields from the bunches, which for small enough size and large enough population cause them to be deflected if they miss each other.[11] The ability to detect this effect determines the size and intensity to be reached in the single beam phase. We shall see that about 5 μm and a few 10^{10} particles is adequate.

Finally we maximize luminosity looking at beam-beam effects in three ways: magnitude of deflection, synchrotron radiation from the collisions (Beamstrahlung)[12] and disruption imaged in the extraction-lines.[13] Detector background[14] minimization is not covered here.

Single Beam Spot Minimization

We first correct anomalous input η. BPMs at the end of the Arc and in the FFS are used to measure beam motion versus energy. This does not give the position-energy correlation within the bunch if anomalous η exists where the energy is varied, but gives a good estimate if the Arc is (as expected) the dominant contributor. As more accuracy is needed, one must constrain η in the Linac or measure spot sizes directly. With 1% energy scans, we determine η to a few mm, or about 5% of the Arc average. Using a model, we determine $\eta_{x,\theta,y,\phi}^{anomalous}$ from a least-square fit to the measurements and calculate the matching solution. Locally orthogonal "knobs" are derived for fine-tweaking. We first correct the β-match, to enable measuring betatron phase space there. Final settings for IP correction will differ if the CCS and Final Demagnifier generate η, for example, through orbit errors. The resulting η_{IP} is mostly spatial as the lenses there are $\pi/2$ phase shift from the IP. Final IP correction is inferred from BPM measurements and from measuring σ^* versus the derived orthogonal knobs, using the wire targets.

Betatron phase space is then diagnosed measuring spot size on a screen versus the strength of an upstream quad, and fitting a parabola.[15] Special emphasis is put on emittance, to help guide tuning in the Arc. Since ϵ enters as a overall scale, we must resolve the parabola's minimum. For a quad and a screen separated by l, this requires $\epsilon l^2/\beta \gg r^2$, where r is the screen resolution. This condition is met before demagnification, in the β-match. A setup with about 100 μm minima in both planes is installed. Twiss parameters, found from the parabola's axis and branches, serve to diagnose gross betatron mismatch. x-y coupling obscuring the ϵ-measurement is diagnosed looking at the tilt of the spot versus quad strength, giving another parabola and three more terms. With nine terms in total, we can in principle fully determine betatron space. In practice, being mostly interested in ϵ, while betatron mismatch is better

measured elsewhere, we simply correct for the measured x-y coupling.

Betatron mismatch is best diagnosed in the Final Demagnifier, where angular and spatial sizes are naturally separated. Using the three β-match knobs, we first set the three angular terms $< \theta^2 >$, $< \phi^2 >$ and $< \theta\phi >$, looking at a nominally round spot on a high-β screen upstream of the Final Triplet. We begin, first ignoring $\epsilon_{x,y}$, by standing the beam upright using the skew quad. Then, taking $\epsilon_{x,y}$ into account, we perturb the two sizes with the erect quads, so as to best satisfy the $\beta^*_{opt} \propto \epsilon^{\frac{1}{3}}$ scaling law (minimizing 3^{rd} order aberration). After this, the beam will have the predicted size at the axial position where it comes to a waist, although that place may be offset from the IP. Correction, amounting to cancel $< x\theta >$, $< y\phi >$ and $< x\phi >$ terms, is calculated sweeping the three Final Triplet knobs and measuring $\sigma^*_{x,y}$ versus strength. As in the phase-space measurement, only the parabola's axis and branches are needed. The axis give the offsets and the branches the derivatives of size versus strength. In principle, resolving the minima is not essential. With all lenses $\pi/2$ from the IP, it can be shown that the skew quad is fully orthogonal to the two other waist controls, provided the $< \theta\phi >$ coupling term is properly nulled; however, the latter two are coupled. The algorithm first orthogonalizes them using the derivatives and then sets them based on the measured axis. The skew quad is adjusted equivalently before or after. η_{IP} can also be cancelled with such parabolic sweeps. Final minimization is achieved iterating all the corrections.

Steering the Beams in Collision

The average mutual deflection of two gaussian beams colliding at an offset Δ is[11]

$$\Theta(\Delta) = \frac{-2r_e N_T}{\gamma} \quad \frac{1 - exp(\Delta^2/2\sigma_T^2)}{\Delta} F(\sigma_P/\sigma_T) \qquad (3)$$

where r_e is the classical electron radius, γ the relativistic factor, N_T the number of particles in the target and $\sigma_{T,P}$ the target and probe sizes. $F(r)=\frac{Ln(1+r^2)}{r^2}$ is a form factor computed for small Δ by folding in the probe distribution. It reduces the average for $\Delta \simeq \sigma$, whereas it should be dropped for $\Delta \gg \sigma$, as the beams then see each other as point charges. Deflection versus offset is shown in Fig. 6 for 50 GeV beams with 5×10^{10} particles and 2, 5 and 10 μm sizes. Detection is best done at the system's high-β points, near the Final Triplet, where it translates into the largest possible shift. Special BPMs are designed[16] for this purpose.

The tuning method proceeds in three steps:

1. *Initial beam finding:* After bringing the beams close with BPMs near the IP, one of them (the most intense) is toggled *on* and *off* while the other is measured at the outgoing high-β point. This gives the shift induced by the collision, the sign telling in which direction to steer. For large Δ and with numerical factors, we get $\delta X_{out}(\mu\text{m}) \approx \frac{70 N_T/5\times10^{10}}{\Delta/100\mu\text{m}}$.

2. *Beam centering:* Scanning one beam across the other enables optimal centering on the zero-deflection symmetry point (see Fig. 6). The largest shift occurs for $\Delta \simeq 1.5\sigma_T$ giving $\delta X^{max}_{out}(\mu\text{m}) \approx \frac{1000 N_T/5\times10^{10}}{\sigma_T/2.5\mu\text{m}}$. With 20 μm measurements and about 2×10^{10} particles initially, we expect good signals for $\sigma \leq 5\mu$m. This sets the goal for single beam optimization.

3. *Feedback:* The mutual deflections are also used to keep the two beams in collision. In simple versions of such feedback, we sample position deviations from an initial reference at reciprocal high-β points on ingoing and outgoing paths. Drifts in the offset are approximated by $\Delta(t) \propto (\delta X_{out}(t) - \delta X_{in}(t))$. A slow

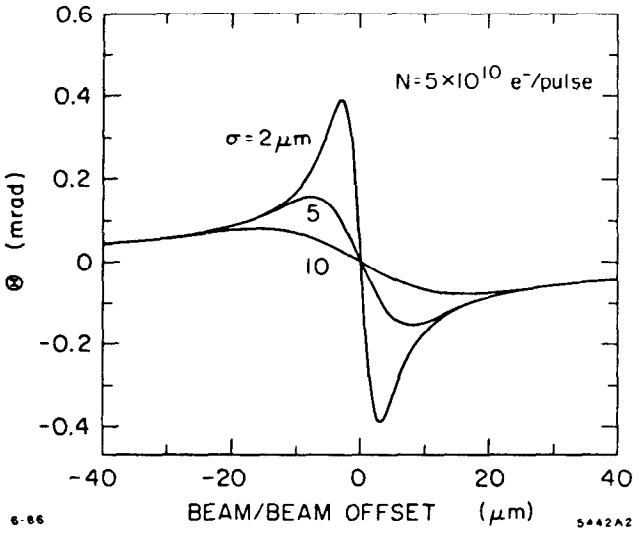

Fig. 6. Beam-beam deflection versus offset for three spot sizes.

version of such a system, with a time constant of about 20 seconds, is available as an extension of existing software.[17] More sophisticated pulse to pulse schemes with optimal filtering[18] of specific frequencies are in progress.

Luminosity Optimization with Beam-Beam Effects

Algorithms based on three beam-beam signals are in progress.

1. *Magnitude of deflection*: The maximum deflection produced in the centering scan is a strong function of beam sizes and can be used for tuning. For centered beams, this signal allows separating improvements in the two planes, but unfortunately not in the two beams. This can be seen noticing that after normalizing by $N_{T,P}$, conservation of the total transverse momentum implies equal average deflections for each beam. The maximum must thus be symmetric in the two beam sizes, making it hard to know which one needs to be optimized (except by sensing derivatives).

2. *Beamstrahlung*:[12] The total photon flux emitted in the collisions is a strong function of beam sizes. For each particle, $N_\gamma \propto \sigma_z/\rho^2 = \theta^2/\sigma_z$, where σ_z, θ and ρ are the bunch-length, deflection angle and radius of curvature. For centered beams of equal size σ_R and populations $N_{1,2}$, Beam 1 radiates $N_\gamma^{total} \propto N_1 N_2^2/\sigma_z\sigma_R^2$. Without the shape of the photon beams it is hard to separate the two planes. One *can* however distinguish the larger from the smaller by scanning one across the other. This is the reversed situation from the deflection signal, making the two methods complementary. The reason is the θ^2-dependence of N_γ, leading to a sum of squares for N_γ^{total}. The dependence of N_γ^{total} from the probe versus Δ is indicated in Fig. 7 for a target with equal, larger or smaller size.

3. *Disruption:* When beams have been made small and intense enough, they act as lenses for each other, thereby increasing their angular spread after collision. In the linear approximation, σ^*_θ grows by about 50% for beams with 2×10^{10} particles and 2 μm transverse sizes. Monitoring of this effect will be possible in the extraction lines, by imaging IP angles on screens through optics designed for the planned energy spectrometers.[13] Tuning for the largest possible spot on these screens will then maximize luminosity.

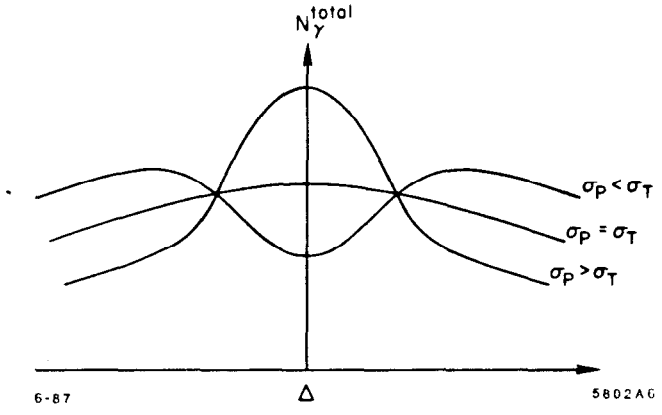

Fig. 7. Total beamstrahlung flux versus offset for unequal transverse beam sizes.

Acknowledgements

I am indebted to several SLC and Mark II colleagues for fruitful discussions. Special credit should be given to K. Brown, T. Fieguth and J. Murray for designing the optics, to W. Kozanecki and R. Erickson for leading our group, and D. Ritson for reviewing many of our algorithms.

References

1. *SLC Design Handbook* (December 1984).
2. J. J. Murray *et al.*, *The Completed Design of the SLC Final Focus System*, these Proceedings.
3. K. L. Brown, private communication (June 1987).
4. J. J. Murray and T. Fieguth, MURTLE, Private Program.
5. K. L. Brown *et al.*, GIAT Committee Report (February 1986).
6. R. V. Servranckx, private communication (June 1987).
7. S. Kheifets *et al.*, *Beam Optical Design and Studies of the SLC Arcs*, SLAC-PUB-4013 (June 1986).
8. K. L. Brown *et al.*, SLAC-91, Rev. 2 (May 1977).
9. E. D. Courant *et al.*, *Theory of the Alternating-Gradient Synchrotron*, Ann. of Phys. 3, 1–48 (1958).
10. L. C. Teng, *Concerning n-Dimensional Coupled Motion*, Fermilab Internal Report FN-229 (May 1971).
11. P. S. Bambade *et al.*, *Beam-Beam Deflection as an Interaction Point Diagnostic for the SLC*, SLAC-PUB-3979 (May 1986).
12. G. Bonvicini *et al.*, *Beamstrahlung Monitor for SLC Final Focus Using Gamma Ray Energies*, SLAC-PUB-3980 (May 1986).
13. Mark II Coll. and SLC Final Focus Group, *Extraction-Line Spectrometers for SLC Energy Measurements*, SLAC-SLC-PROP(2) (1986).
14. W. Kozanecki, GIAT Committee Report (January 1986).
15. M. C. Ross *et al.*, *High Resolution Beam Profile Monitors in the SLC*, SLAC-PUB-3640 (April 1985).
16. J. C. Denard *et al.*, *Monitoring the Beam Position in the SLC Interaction Region*, these Proceedings.
17. K. A. Thompson *et al.*, *Feedback Systems in the SLC*, these Proceedings.
18. R. Stiening, *Sampled Feedback in the Linear Collider*, SLAC CN-14 (November 1980).